19

Metal-Organic Polyhedra and Covalent Organic Polyhedra

19.1 Introduction

Reticular chemistry is concerned with linking molecular building units through strong bonds into predefined structures [1]. Most products of reticular synthesis are 2D or 3D extended frameworks; however, this chemistry can further be applied to target the formation of discrete 0D compounds. In the following text, we describe how the design principles that we have covered in the context of metal-organic frameworks (MOFs) and covalent organic frameworks (COFs) can be applied to the synthesis of metal-organic polyhedra (MOPs) and covalent organic polyhedra (COPs)–discrete intrinsically porous cage compounds [2]. We limit the discussion to porous cage compounds that sustain permanent porosity and whose structures are unambiguously confirmed by X-ray diffraction. With respect to MOPs only structures based on secondary building units (SBUs) are discussed. For further information on coordination cages based on single metal nodes the reader is referred to the literature [3]. For COPs the discussion is limited to structures based on linkage chemistries utilized in COF chemistry and for other shape-persistent organic cages we refer the reader to the literature [4].

19.2 General Considerations for the Design of MOPs and COPs

The nine different shapes of polyhedra that are most likely to form as products of reticular synthesis of MOPs and COPs are the edge-transitive convex polyhedra that have already been described in Chapter 18. They can be divided into (i) Vertex-, face-, and edge-transitive regular polyhedra (tetrahedron, octahedron, cube, icosahedron, and dodecahedron); (ii) quasiregular polyhedra, which are edge and vertex transitive but have two kinds of face (triacontahedron and icosidodecahedron), and (iii) the duals of these two quasiregular polyhedra, which are edge and face transitive but have two kinds of vertex (rhombic dodecahedron and octahedron) [5]. The topology can give an idea about the connectivity the building units must have to target polyhedra carrying their respective nets. However this knowledge alone does not suffice to specifically target MOPs and

Introduction to Reticular Chemistry: Metal-Organic Frameworks and Covalent Organic Frameworks,
First Edition. Omar M. Yaghi, Markus J. Kalmutzki, and Christian S. Diercks.

Companion website: www.wiley.com/go/yaghi/reticular

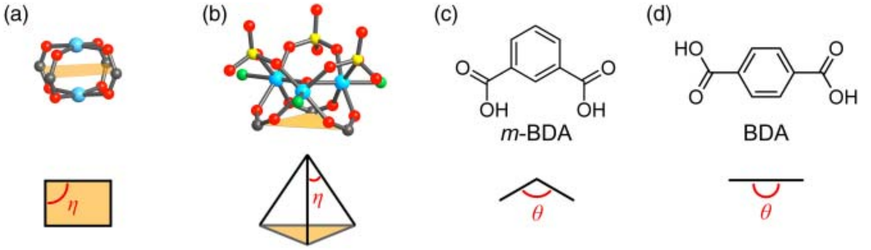

Figure 19.1 Illustration of the angles η in the molecular building units that form the vertices and the angle θ of the linkers representing the edges of the targeted topology. (a) The angle η in a $Cu_2(–COO)_4$ copper paddle wheel SBU. (b) The angle η in an $Fe_3OL_3(–COO)_3(SO_4)_3$ SBU. (c) The angle θ in *m*-BDC, and in BDC (d). All hydrogen atoms are omitted for clarity. Color code for (a, b): M, blue; C, gray; O, red; S, yellow; N, green.

COPs because the competitive formation of extended 2D and 3D frameworks with the same connectivity is generally more favorable. Hence, the formation of MOPs and COPs requires the judicious choice of both the angle θ between the points of extension of the molecules that represent the edges (linkers with two points of extension) and the angle η between the respective points of extension of the vertex (SBU or linker with more than two points of extension) as illustrated in Figure 19.1 [2].

In this chapter, selected examples for the synthesis of MOPs and COPs representing different polyhedra are highlighted and geometric requirements for the building units deciphered.

19.3 MOPs and COPs Based on the Tetrahedron

To target MOPs or COPs with an underlying tetrahedron (**tet**) topology, four 3-c SBUs with angle η need to be joined by six ditopic linkers with angle θ. In Figure 19.2 the two extreme scenarios of configurations that can lead to a tetrahedron are illustrated: (i) $\eta = 60°$, $\theta = 180°$ and (ii) $\eta = 120°$, $\theta = 70.5°$. These are the angles for the two idealized extreme conformations that a tetrahedron can assume and, of course, in reality the angles found in structures of this topology are typically somewhere between these values. Nonetheless, the idealized structures serve as a valuable reference for targeting MOPs and COPs of **tet** topology.

An isoreticular series of MOPs assuming a conformation close to the first extreme case of a tetrahedron (i) is constructed from partially sulfate-capped $Fe_3OL_3(–COO)_3(SO_4)_3$ SBUs connected by linear ditopic BDC, BPDC, and BPTC to yield IRMOP-50, IRMOP-51, and IRMOP-53, respectively (Figure 19.3) [6]. In this series, the pore size in the center of the tetrahedron is varied systematically: 7.3, 10.4, and 13.3 Å for IRMOP-50, IRMOP-51, and IRMOP-53, respectively. The surface area of IRMOP-51 determined by nitrogen adsorption is calculated to be $480\,m^2\,g^{-1}$. In contrast, the isoreticular expanded IRMOP-53 has a lower surface area of just $387\,m^2\,g^{-1}$. This appears counterintuitive at first but can be rationalized by the fact that for the case of discrete 0D polyhedra not only the intrinsic pore of the cage is relevant to the surface area but also the

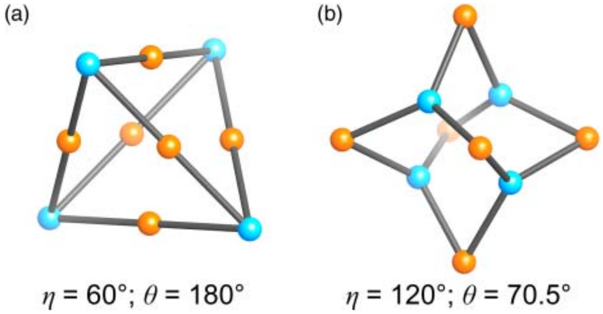

Figure 19.2 Two extreme cases of four 3-c vertices linked by edges to form a tetrahedron. (a) One extreme case is the linking of vertices with the minimum angle of $\eta = 60°$ with linear edges of $\theta = 180°$. (b) In the second extreme case the vertices have the maximum angle of $\eta = 120°$ and an angle of $\theta = 70.5°$. In reality, the angles are found somewhere between these values. Color code: vertices, blue; edges, orange.

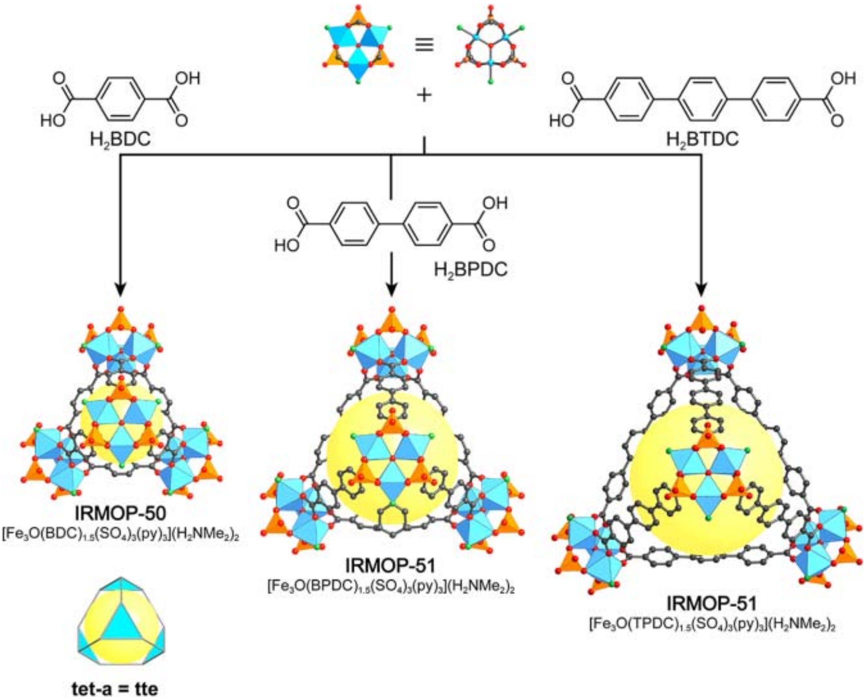

Figure 19.3 MOPs assuming a tetrahedron topology. Partially sulfate capped $Fe_3OL_3(-COO)_3(SO_4)_3$ SBUs are linked by linear ditopic BDC, BPDC, and TPDC to yield an isoreticular series of MOPs termed IRMOP-50, IRMOP-51, and IRMOP-53, respectively. All hydrogen atoms are omitted for clarity. Color code: Fe, blue; S, orange; C, gray; N, green; O, red.

extrinsic pores resulting from how the molecular cages are packed in the solid state. In IRMOP-51, 76% of the crystal structure is free volume as opposed to only 70.5% in IRMOP-53, and consequently the higher surface area of IRMOP-51 is rationalized by the additional uptake in the extrinsic pores of the crystal.

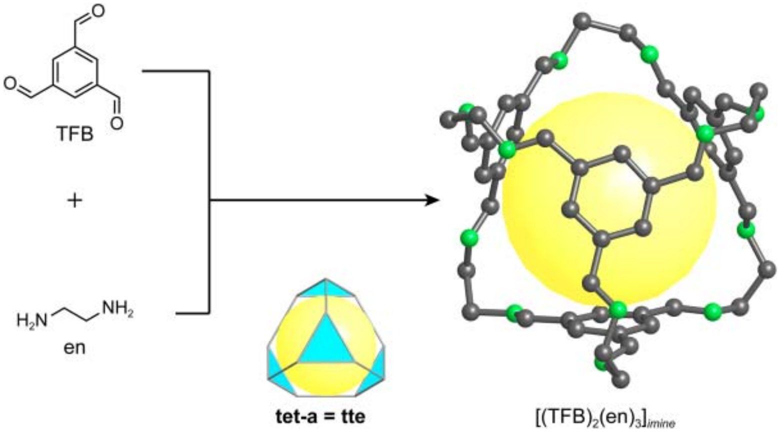

Figure 19.4 Reticulation of TFB with en yields the **tet** topology COP $[(\mathrm{TFB})_2(\mathrm{en})_3]_{imine}$, which resembles the second extreme case for the tetrahedron with angles $\eta = 118°$, $\theta = 74.5°$. In the crystal structure the cages pack in a face-sharing manner to yield a structure of **dia** topology held together by weak interactions. All hydrogen atoms are omitted for clarity. Color code: C, gray; N, green.

The other extreme scenario is exemplified by a COP constructed from tritopic TFB with ditopic en (1,2-ethylene diamine) of molecular formula $[(\mathrm{TFB})_2(\mathrm{en})_3]_{imine}$ (Figure 19.4) [7]. In this structure, the angles, $\eta = 118°$, $\theta = 74.5°$ are close to the values in the second extreme conformation of the tetrahedron (Figure 19.2b). The pore size of the cage has a diameter of 7.8 Å and in the crystal structure its trigonal faces are packed in a face-to-face manner to yield channels of 5.8 Å. The packing resembles a diamond-like arrangement of the COPs with an interconnected pore system that endows the material with a BET surface area of $624\,\mathrm{m}^2\,\mathrm{g}^{-1}$.

19.4 MOPs and COPs Based on the Octahedron

MOPs and COPs based on the octahedron are composed of six 4-c vertices with angle η joined by links with angle θ. There are two extreme cases of configurations: (i) $\eta = 60°$, $\theta = 180°$ and (ii) $\eta = 90°$, $\theta = 90°$ (Figure 19.5).

As of now, no MOP or COP resembling the extreme case (i) is known in the literature. An example for the second type of configuration is the structure of MOP-28 (Figure 19.6) [8]. The cage is constructed from $\mathrm{Cu}_2(\mathrm{-COO})_4$ paddle wheel SBUs linked by bent $\mathrm{H}_2\mathrm{TTC}$ (2,2′:5′,2″-terthiophene-5,5″-dicarboxylic acid) linkers. In the crystal structure the copper paddle wheels are slightly distorted but maintain an average angle of $\eta = 90°$. The TTC linkers also have the ideal angle of $\theta = 90°$ found in the second extreme case of an octahedron. The pore size of MOP-28 is 27.0 Å with large, 9 Å wide pore openings. The structure is architecturally stable and sustains permanent porosity with a surface area of $1100\,\mathrm{m}^2\,\mathrm{g}^{-1}$.[1] It is important to consider that discrete porous cages often lose

---

[1] This is the first MOP that was proved to sustain permanent porosity.

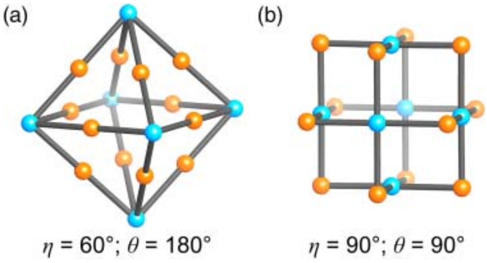

Figure 19.5 Two extreme cases of 6 4-c vertices linked by 12 edges to form an octahedron. (a) One extreme case is the linking of vertices with the minimum angle of $\eta = 60°$ with linear edges of $\theta = 180°$. (b) In the second extreme case the vertices have the maximum angle of $\eta = 90°$ and an angle of $\theta = 90°$. The angles in synthetic structures are found within these boundaries. Color code: vertices, blue; edges, orange.

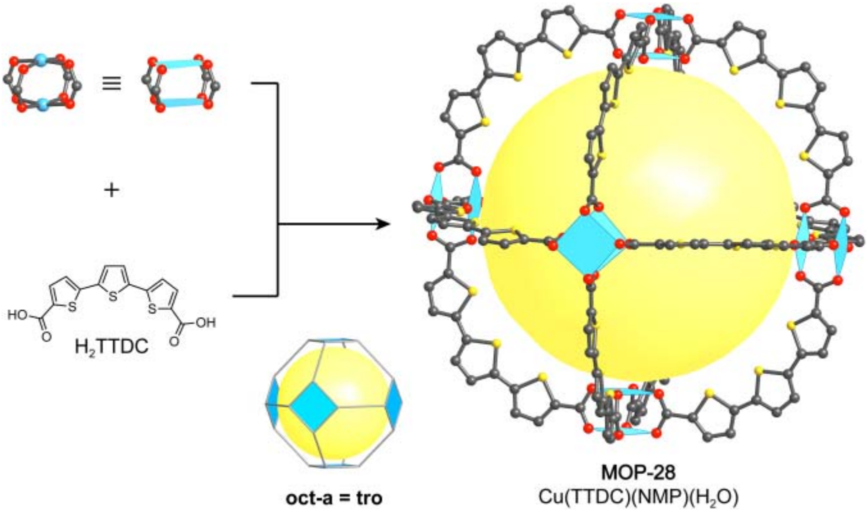

Figure 19.6 The structure of MOP-28, an example of a MOP in the shape of an octahedron. The averaged angles within the $Cu_2(-COO)_4$ paddle wheel of $\eta = 90°$ and the $\theta = 90°$ angles between the points of extension of the bent ditopic TTDC linker perfectly match the angles of the second extreme case of a cube (Figure 19.5b). All hydrogen atoms are omitted for clarity. Color code: Cu, blue; C, gray; O, red; S, yellow.

porosity upon cycling due to changes in the crystal packing but in the case of MOP-28 no decrease in nitrogen uptake or in surface area is detected.

19.5 MOPs and COPs Based on Cubes and Heterocubes

In cubes eight 3-c vertices with angle η are joined by ditopic edges with an angle θ. The two extreme cases are formed with angles (i) $\eta = 90°$, $\theta = 180°$ and (ii) $\eta = 120°$, $\theta = 109.5°$ (Figure 19.7).

While there are several coordination cages (polyhedra based on single-metal nodes) that assume the first of the two extreme cases of an octahedron, no MOPs

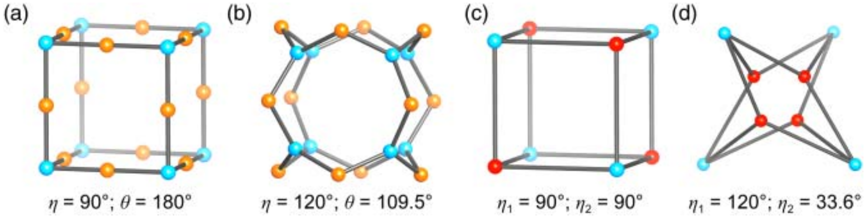

Figure 19.7 (a, b) Two extreme cases to construct cubes from 8 3-c vertices and 12 edges: (a) $\eta = 90°$ and $\theta = 180°$, (b) $\eta = 120°$ and edges $\theta = 109.5°$. (c, d) Construction of heterocubes each built from two sets of four respective 3-c vertices. There are two extreme cases: (c) $\eta = 90°$ and $\theta = 90°$, (d) $\eta = 120°$ and $\theta = 33.6°$. Color code: vertices, blue or red; edges, orange.

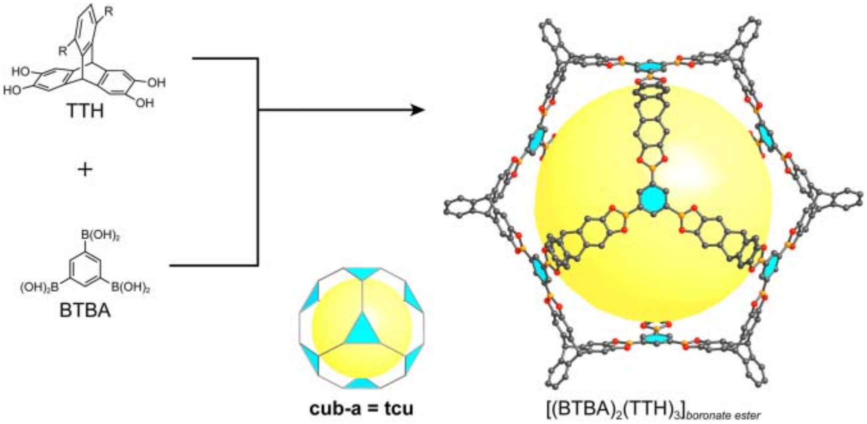

Figure 19.8 Synthesis of $[(\text{BTBA})_2(\text{TTH})_3]_{boronate\ ester}$, a mesoporous COP. Reticulation of trigonal tritopic BTBA with linear ditopic TTH yields a cage similar to that of the second extreme case for the conformation of cubes. The angles $\eta = 118°$ and edges $\theta = 110°$ are very close to the idealized angles. All hydrogen atoms are omitted for clarity. Center of the tritopic linker, blue; B, orange; C, gray; O, red.

are known. For examples on single-metal coordination cages we refer the reader to the literature [9].

An example for the second extreme case of a cube is found in the boronate ester-linked COP $[(\text{BTBA})_2(\text{TTH})_3]_{boronate\ ester}$ (BTBA = benzene-1,3,5-triyltriboronic acid, TTH = ((9s,10s)-13,16-diethyl-9,10-dihydro-9,10-[1,2] benzenoanthracene-2,3,6,7-tetraol). In its structure, 8 BTBA and 12 TTH are linked by boronate ester bonds (Figure 19.8) [10]. The resulting COP has a large pore of 2.4 nm diameter and can be activated to yield a permanently mesoporous cage with an exceptionally high surface area of 3758 $m^2\ g^{-1}$. Depending on the functionalization pattern of the TTH building unit, a catenated version of $[(\text{BTBA})_2(\text{TTH})_3]_{boronate\ ester}$ is isolated where two cages quadruply interlock to yield a catenane in high yield (62%). This is interesting because in general the formation of catenanes or related interlocking molecules requires a template to obtain them in high yield. Multicomponent reactions such as the 96-fold

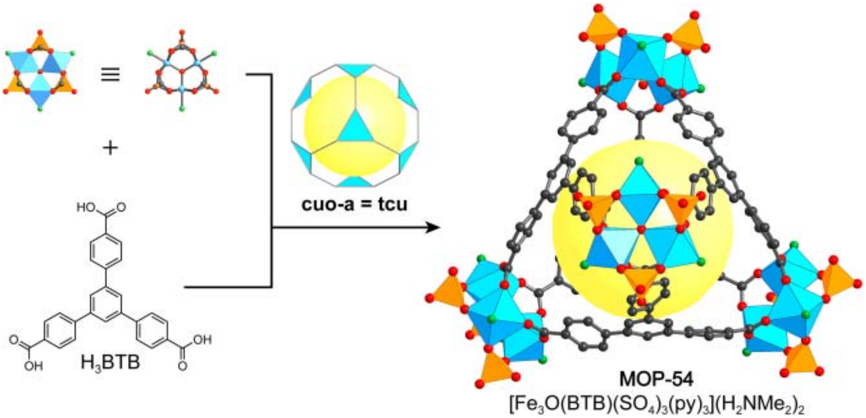

Figure 19.9 Synthesis of a MOP heterocube. Reticulation of H_3BTB with Fe^{2+} yields MOP-54. The angle $\eta_1 = 113°$ in the BTB linker and $\eta_2 = 67.1°$ in the SBU deviate substantially from the values of the idealized two extreme cases for a heterocube. All hydrogen atoms are omitted for clarity. Color code: Fe, blue; S, orange; C, gray; N, green; O, red.

boronate ester bond formation in this example further complicate their formation. This phenomenon is reminiscent of the interpenetration of 2D and 3D frameworks and is likely thermodynamically favorable as no large open pores are generated during the synthesis [11].

Another way to construct cube-shaped MOPs is by making so-called heterocubes, where two different trivalent SBUs with links of angles η_1 and η_2 are joined together. Here again, there are two extreme scenarios: (i) $\eta_1 = \eta_2 = 90°$ and (ii) $\eta_1 = 120°$ and $\eta_2 = 33.6°$ (Figure 19.7c,d).

An example for the second extreme case of a heterocube is MOP-54, constructed from partially sulfate-capped $Fe_3OL_3(-COO)_3(SO_4)_3$ SBUs and trigonal tritopic BTB linkers (Figure 19.9). The structure of MOP-54 is related to the structures of IRMOP-50, IRMOP-51, and IRMOP-53, yet topologically they are fundamentally different. While in the case of the IRMOP series six linear ditopic linkers are lying on the edges of a tetrahedron formed by four SBUs, in the case of MOP-54 four trigonal tritopic linkers occupy the faces of the tetrahedron. Topologically the IRMOP series are tetrahedra, whereas MOP-54 is classified as a heterocube. The structure resembles more the second extreme case of a heterocube despite significant deviations from the idealized angles ($\eta_1 = 113°$; $\eta_2 = 67.1°$) (see Figure 19.7d) [6]. This example highlights that in some cases strong structural similarities may be lost in the topological description of reticular materials and, as such, topology should only serve as a tool and by no means as a replacement for a deep understanding of the chemical nature of a given material.

19.6 MOPs Based on the Cuboctahedron

In a cuboctahedron, 12 4-c vertices are joined by 20 ditopic edges. The two extreme cases are shown in Figure 19.10. In the first case the edges are straight

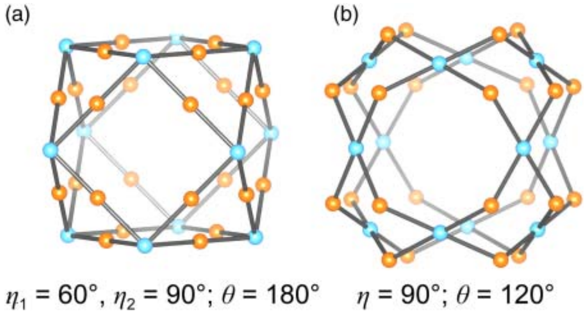

$\eta_1 = 60°, \eta_2 = 90°; \theta = 180°$ $\eta = 90°; \theta = 120°$

Figure 19.10 Two extreme cases of 12 4-c vertices linked by 20 edges to form a cuboctahedron. (a) One extreme case is the linking of vertices with the minimum angle of $\eta_1 = 60°$ and $\eta_2 = 90°$ with linear edges of $\theta = 180°$. (b) In the second extreme case the vertices have the maximum angle of $\eta = 90°$ and an angle of $\theta = 117°$. Color code: vertices, blue; edges, orange.

(θ = 180°), and the tetravalent vertices are not at sites of fourfold symmetry and thus it is no longer possible to give a single value of η to relate the angles. Consequently, there are two kinds of angle between the edges from the center of the vertices of $\eta_1 = 60°$ and $\eta_2 = 90°$ (Figure 19.10a). In the second case, the angle between the square planar vertices are $\eta_1 = 90°$ and the edges are bent to an angle of $\theta = 117°$ (Figure 19.10a).

MOP-1 is constructed from $Cu_2(-COO)_4$ paddle wheel SBUs linked by bent *m*-H_2BDC linkers. The 90° angles in the paddle wheel SBUs and the 120° angles in the *m*-BDC linker are almost identical to the idealized second extreme case with 90° angles between the points of extension of the paddle wheel SBU and 120° angles between the carboxylate carbons of the linker (Figure 19.10b). MOP-1 has already been discussed in Section 4.2.2 in the context of the influence of linker geometry on the linking of paddle wheel SBUs (Figure 19.11). It is worthwhile

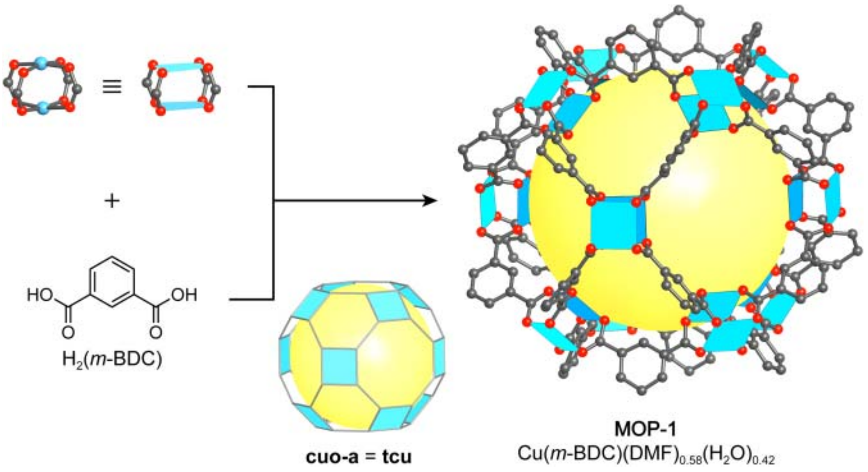

Figure 19.11 The cuboctahedral MOP-1 is constructed from $Cu_2(-COO)_4$ paddle wheel SBUs and bent *m*-H_2BDC linkers. The angles in the SBU and the linker are identical to those in the idealized extreme case 2 with $\eta = 90°$ and $\theta = 120°$. All hydrogen atoms are omitted for clarity. Color code: Cu, blue; C, gray; O, red.

mentioning that MOPs such as MOP-1 are used as tertiary building units in the synthesis of complex hierarchical MOFs.

19.7 Summary

In this chapter, we covered the reticular synthesis of MOPs and COPs and outlined the necessary structural requirements imposed on the building units to selectively target the formation of these discrete compounds over their extended counterparts, MOFs and COFs. We have discussed the angles η and θ between the points of extension of the building units representing the vertex and the edge of the underlying topology, respectively. The two extreme cases that these two angles can assume in MOPs and COPs of **tet**, **oct**, **cub**, and **cuo** topologies were shown and illustrative examples of polyhedra of these structure types were given and their angular information examined. Finally, important considerations with respect to the surface area of discrete polyhedra were covered and the interplay between intrinsic surface area of the polyhedra and the extrinsic surface area imposed by the packing of these discrete molecules in the crystal structure were discussed.

References

1 (a) Diercks, C.S. and Yaghi, O.M. (2017). The atom, the molecule, and the covalent organic framework. *Science* 355 (6328): eaal1585. (b) Yaghi, O.M., O'Keeffe, M., Ockwig, N.W. et al. (2003). Reticular synthesis and the design of new materials. *Nature* 423 (6941): 705–714. (c) Furukawa, H., Cordova, K.E., O'Keeffe, M., and Yaghi, O.M. (2013). The chemistry and applications of metal-organic frameworks. *Science* 341 (6149): 1230444.

2 Tranchemontagne, D.J., Ni, Z., O'Keeffe, M., and Yaghi, O.M. (2008). Reticular chemistry of metal-organic polyhedra. *Angewandte Chemie International Edition* 47 (28): 5136–5147.

3 (a) Fujita, M. (1998). Metal-directed self-assembly of two-and three-dimensional synthetic receptors. *Chemical Society Reviews* 27 (6): 417–425. (b) Seidel, S.R. and Stang, P.J. (2002). High-symmetry coordination cages via self-assembly. *Accounts of Chemical Research* 35 (11): 972–983. (c) Caulder, D.L. and Raymond, K.N. (1999). Supermolecules by design. *Accounts of Chemical Research* 32 (11): 975–982. (d) Han, M., Engelhard, D.M., and Clever, G.H. (2014). Self-assembled coordination cages based on banana-shaped ligands. *Chemical Society Reviews* 43 (6): 1848–1860.

4 (a) Mastalerz, M. (2010). Shape-persistent organic cage compounds by dynamic covalent bond formation. *Angewandte Chemie International Edition* 49 (30): 5042–5053. (b) Zhang, G. and Mastalerz, M. (2014). Organic cage compounds – from shape-persistency to function. *Chemical Society Reviews* 43 (6): 1934–1947. (c) Hasell, T. and Cooper, A.I. (2016). Porous organic cages: soluble, modular and molecular pores. *Nature Reviews Materials* 1 (9): 16053.

5 (a) Delgado-Friedrichs, O., O'Keeffe, M., and Yaghi, O.M. (2007). Taxonomy of periodic nets and the design of materials. *Physical Chemistry Chemical*

Physics 9 (9): 1035–1043. (b) Ockwig, N.W., Delgado-Friedrichs, O., O'Keeffe, M., and Yaghi, O.M. (2005). Reticular chemistry: occurrence and taxonomy of nets and grammar for the design of frameworks. *Accounts of Chemical Research* 38 (3): 176–182.

6 Sudik, A.C., Millward, A.R., Ockwig, N.W. et al. (2005). Design, synthesis, structure, and gas (N_2, Ar, CO_2, CH_4, and H_2) sorption properties of porous metal-organic tetrahedral and heterocuboidal polyhedra. *Journal of the American Chemical Society* 127 (19): 7110–7118.

7 Tozawa, T., Jones, J.T., Swamy, S.I. et al. (2009). Porous organic cages. *Nature Materials* 8 (12): 973–978.

8 Ni, Z., Yassar, A., Antoun, T., and Yaghi, O.M. (2005). Porous metal-organic truncated octahedron constructed from paddle-wheel squares and terthiophene links. *Journal of the American Chemical Society* 127 (37): 12752–12753.

9 Liu, Y., Kravtsov, V., Walsh, R.D. et al. (2004). Directed assembly of metal-organic cubes from deliberately predesigned molecular building blocks. *Chemical Communications* (24): 2806–2807.

10 Zhang, G., Presly, O., White, F. et al. (2014). A permanent mesoporous organic cage with an exceptionally high surface area. *Angewandte Chemie International Edition* 53 (6): 1516–1520.

11 Zhang, G., Presly, O., White, F. et al. (2014). A shape-persistent quadruply interlocked giant cage catenane with two distinct pores in the solid state. *Angewandte Chemie International Edition* 53 (20): 5126–5130.